SUPPLEMENTARY METHODS

In silico modeling

Simulation studies were conducted using a population of virtual human atrial models based on the Maleckar *et al.* model (*41*), which yields an AP morphology closely resembling the human atrial APs recorded in this study. The model incorporates biophysically-detailed descriptions of the main transmembrane ionic currents, ion homeostasis and intracellular Ca^{2+} handling of the human atrial myocyte. Briefly, an initial population of 30,000 human atrial models was generated as in (*17*). For every model within the initial cell population, simulations were conducted using voltage clamp protocols and stimulation trains of 100 beats at five pacing frequencies (0.25, 0.5, 1, 2, and 3 Hz) using identical protocols, as in the patch clamp experiments. Electrophysiological properties were calculated for each model at all pacing frequencies, including the magnitude of each ionic current as measured in voltage clamp, AP amplitude, APD_{50} and AD_{90}, AP triangulation and resting membrane potential. From the initial 30,000 sampled models, the experimentally-calibrated population of human atrial models was constructed by retaining only the models yielding values for all ionic currents and AP properties within the range obtained experimentally in SR. The resultant experimentally-calibrated SR population consisted of 640 human atrial models. The SR population was used to investigate the role of SMTC-induced changes in I_{to}, I_{Kur}, $I_{Ca,L}$ and I_{K1} in recovering APD changes measured experimentally.

SUPPLEMENTARY FIGURES

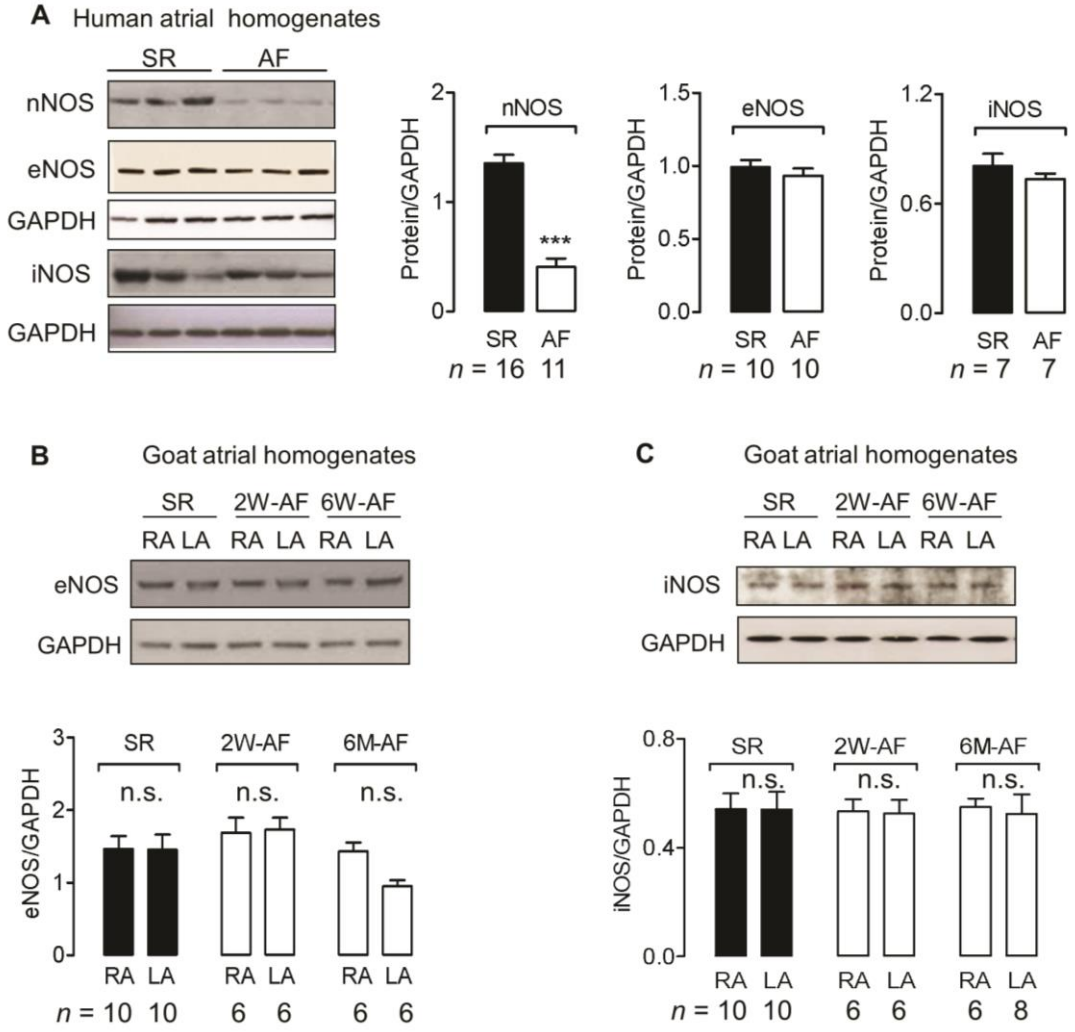

Fig. S1. NOS isoforms in human and goat atrial tissue. (**A**) Protein content of nNOS, eNOS or iNOS in human right atrial (RA) tissue, or in goat RA and left atrial (LA) tissue (**B, C**); normalized to GAPDH. Data were averages ± SEM. ***$P < 0.001$ *vs* SR, unpaired *t* test (**A**) or 1-way ANOVA with Bonferroni correction (**B** and **C**).

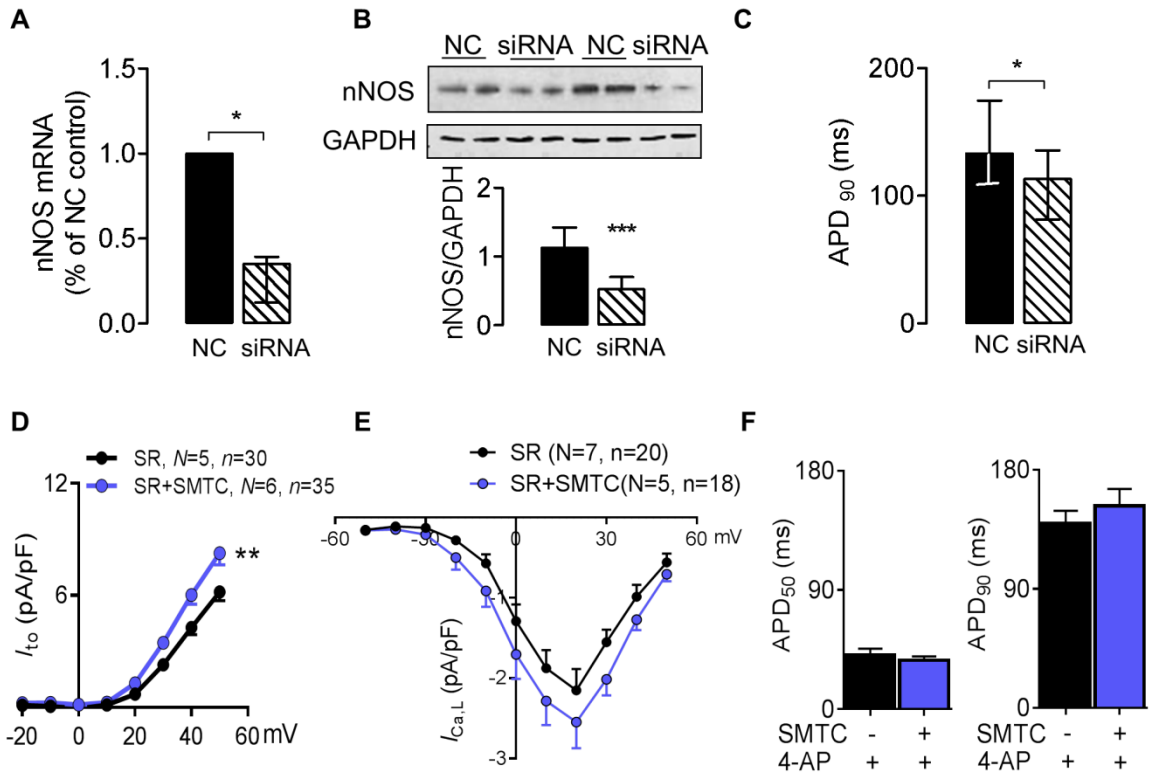

Fig. S2. **nNOS knock-down or pharmacological inhibition in human atrial myocytes.**
(**A** to **C**) Gene expression (**A**, *n* = 10 / group), GAPDH-normalized protein content (**B**, *n* = 8 / group), and APD_{90} (**C**) in human right atrial myocytes obtained from patients in SR after knockdown of nNOS mRNA with Accell SMARTpool siRNA (1 µM for ~80 hours). Gene expression was normalized to *GAPDH* and expressed as a percentage of the respective non-targeting control (NC; Dharmacon). Data are medians and interquartile ranges (IQR) in **A** and **C** and averages ± SEM in **B**. * *P* <0.001 *vs* SR, Wilcoxon signed rank test (**A**), ***$P < 0.001$, paired *t* test (**B**) or *P* = n.s., Mann-Whitney *U* test (**C**). (**D**) Current-voltage relationships (averages ± SEM) for I_{to} in atrial myocytes from patients in SR, in the presence or absence of nNOS inhibition with SMTC. ** $P < 0.01$ for the interaction between SMTC and voltage, two-way ANOVA. (**E**) Current–voltage relationships (averages ± SEM) for the L-type calcium current, $I_{CaL,}$ in the presence or absence of nNOS inhibition. *P* = 0.12 for the effect of SMTC, 2-way repeated measure ANOVA. N, number of patients; n, number of cells. **(F)** Effect of inhibiting I_{Kur} with 4-aminopiridine (4-AP, 50 µM) on the APD_{50} and APD_{90} response to SMTC (4-AP: *n* = 22 cells from 9 patients; 4-AP+SMTC: *n* = 17 cells from 7 patients). Data are averages ± SEM.

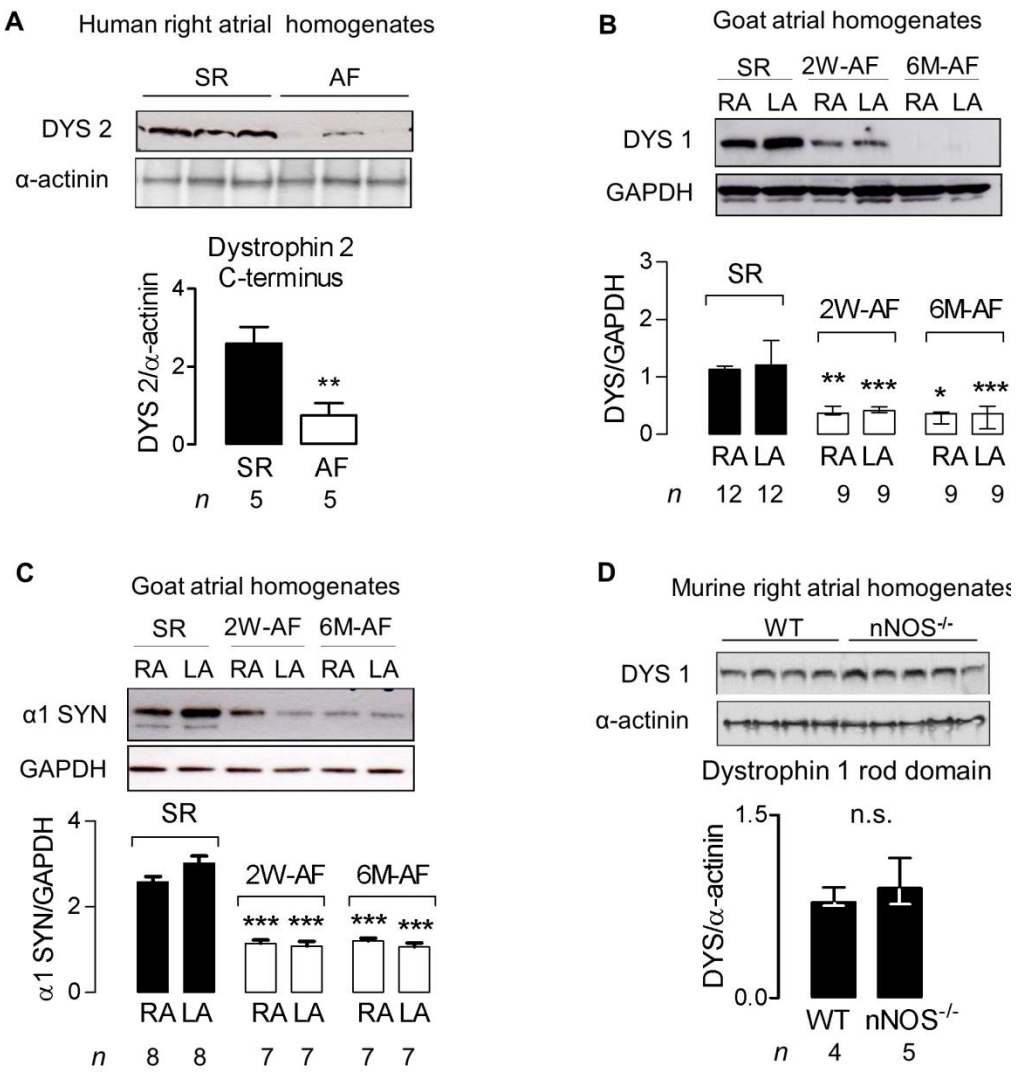

Fig. S3. Atrial content of dystrophin and dystrophin-associated proteins in SR and AF. (**A**) Atrial dystrophin (DYS) content in patients with AF or SR (probed with antibody raised against the C-terminus). Protein content is normalized to GAPDH. Data are averages ± SEM. $^{**}P < 0.01$, unpaired *t* test. (**B** and **C**) Right (RA) and left atrial (LA) DYS and α1 syntrophin (SYN) content (normalized to GAPDH) in goats after 2 weeks (2W) and 6 months (6M) of AF compared with animals in SR. Data are averages ± SEM. $^{*}P < 0.05$, $^{**}P < 0.01$, $^{***}P < 0.001$ *vs* SR, Kruskal-Wallis (**B**) or 1-way ANOVA with Bonferroni correction (**C**). (**D**) Effect of *nNos* gene deletion on atrial dystrophin content (normalized to α-actinin) in mice. Data are medians and IQR. *P* = n.s., Mann-Whitney *U* test

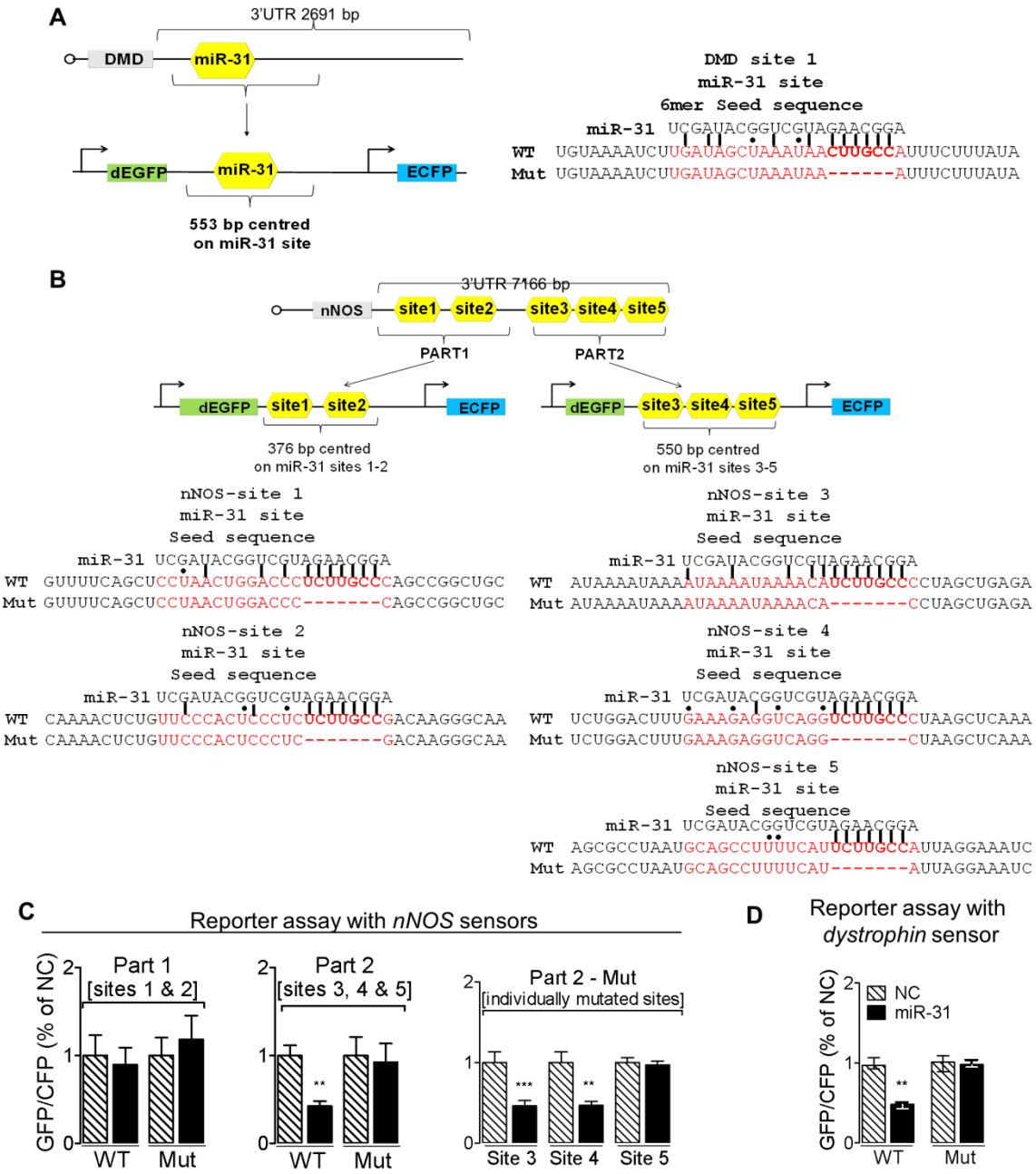

Fig. S4. Reporter assay with dystrophin and nNOS sensors. (**A** and **B**) Schematic representation of the constructs for dystrophin (DMD) and nNOS reporters with miR-31 binding sites (in yellow); mutations raised are shown in red and the seed sequence is in bold red. (**C** and **D**) HEK293T cells were co-transfected with either a miR-31 mimic or a non-targeting negative control #1 (NC, Dharmacon) and with reporters containing nNOS or dystrophin 3'UTR fragments with wild type (WT) or mutated (Mut) putative binding sites for miR-31 (*n* = 6-12 biological replicates per group). The effect of the miR-31 mimic was normalized to the NC. Data are averages ± SEM (**C**) or medians and IQR (**D**). ***P* < 0.01, ****P* < 0.001 *vs* the WT construct, 1-way ANOVA after log transformation (**C**) or Kruskal-Wallis with Dunn's correction (**D**).

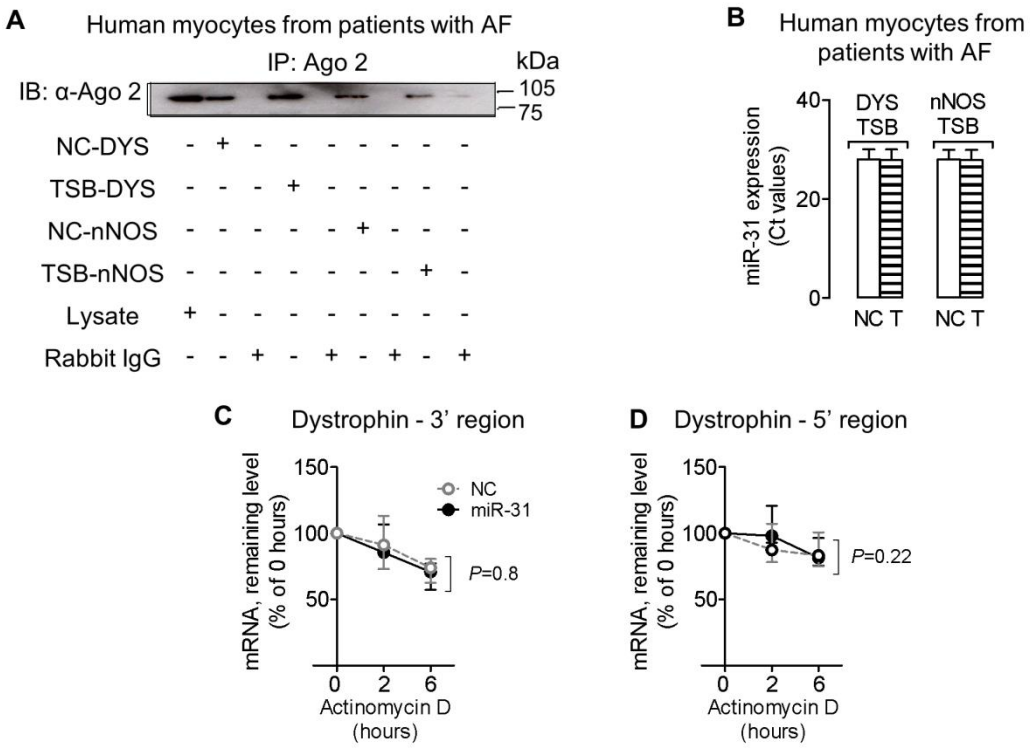

Fig. S5. MiR-31 in Ago-2 immunoprecipitates and effect of miR-31 mimic on the dystrophin mRNA decay. (**A**) Representative immunoblots showing Ago-2 immunoprecipitation in atrial myocytes isolated from patients with AF and transfected with a dystrophin or nNOS target site blocker (TSB-DYS or TSB-nNOS), or with the respective non-targeting negative control #1 (NC, Dharmacon). Myocytes lysate and rabbit (Rb) IgG were used as controls for the efficiency of immunoprecipitation and for non-specific binding, respectively. (**B**) miR-31 expression in Ago2-immunoprecipitates was quantified by qRT-PCR and expressed as Ct values (n = 9 in each group).Data are averages ± SEM; P = n.s., unpaired t test. (**C, D**) Effect of miR-31 mimic on DYS mRNA decay in actinomycin D-treated atrial myocytes from patients in SR (n = 4-6). Primers for 3' or 5' regions of the dystrophin transcript were used in C and D respectively. DYS mRNA was normalized to GAPDH and expressed as % of control at 0 hours. Data are averages ± SEM; P = n.s., by 2-way ANOVA with Bonferroni correction.

SUPPLEMENTARY TABLES

Table S1. Clinical and demographic characteristics of patients in SR and with persistent AF. ACEI, angiotensin-converting enzyme inhibitor; AF, atrial fibrillation; ARB, angiotensin II receptor blocker; AVR, aortic valve replacement; CABG, coronary artery bypass surgery; CCB, calcium channel blocker; COPD, chronic obstructive pulmonary disease; MI, myocardial infarction; MVR, mitral valve replacement; SR, sinus rhythm. The χ^2 test was use to compare gender, smoking status, and medical history between groups; the unpaired *t* test was used to compare age and the Fisher's exact test for surgical procedures. .

Groups of comparison	**SR**	**Persistent AF**	**P value**
Total number patients, *n*	(n = 176)	(n = 51)	
Age, years (mean ± SD)	69±10	73±10	0.0009
Men, n %	123 (70)	33 (65)	0.76
Surgical procedure, %			
CABG±AVR/MVR	125 (71)	17 (33)	0.01
AVR/MVR	51 (29)	27 (53)	0.05
Maze procedure	0 (0)	7 (14)	<0.0001
Medical history, n %			
Smoker/ex-smoker	99 (56)	21 (41)	0.27
Hypertension	130 (74)	31 (61)	0.44
Diabetes mellitus	39 (22)	6 (12)	0.17
Heart Failure	42 (24)	18 (35)	0.22
Previous MI	55 (31)	2 (4)	0.001
COPD/asthma	12 (7)	6 (12)	0.38
Medications, %			
Anticoagulants	16 (9)	33 (64)	<0.0001
Antiplatelets	127 (72)	11 (22)	0.0003
β-blockers	100 (57)	23 (45)	0.68
Statins	128 (73)	25 (49)	0.14
CCB	35 (20)	6 (12)	0.26
ACEIs and ARBs	97 (55)	22 (43)	0.39
Diuretics	48 (27)	22 (43)	0.13

Table S2. Action potential characteristics of human and murine right atrial myocytes in the presence of absence of nNOS inhibitor SMTC. Data are averages ± SEM. *n*, number of myocytes; *N,* number of animals or patients.

	Human				**Mouse**		
	SR *n/N*=52/14	SR + SMTC n/N=45/12	AF *n/N*=40/13	AF + SMTC *n/N*=27/6	WT *n/N*=18/6	WT + SMTC *n/N*=9/4	*nNos*$^{-/-}$ *n/N*=28/9
Resting membrane potential (mV)	-75.5 ± 0.5	-76.4 ± 0.7	-74.9 ± 0.7	-73.1 ± 1.3	-72.1 ± 0.7	-72.4 ± 1.9	-72.6 ± 1.1
Action potential amplitude (mV)	116.7 ± 1.2	113.1 ± 1.4	114.7 ± 1.7	117.4 ± 1.7	119.7 ± 2.8	122.9 ± 2.7	120.3 ± 2.5

Table S3. *In vivo* cardiac electrophysiological parameters of WT and *nNos*$^{-/-}$ mice. RR interval is the interval between two consecutive R waves of the QRS complex (used to assess the ventricular rate);whereas, the PQ interval is the period that extends from the beginning of the P wave until the beginning of the QRS complex; sinus node recovery time is the interval between the last paced P wave and the following sinus P wave; atrio-ventricular Wenck interval is the cycle length at which atrio-ventricular Wenckebach block occurs during atrial pacing. Atrio-ventricular effective refractory period is defined by the shortest S1-S2 interval blocking atrio-ventricular conduction during atrial pacing. *P* values were determined using two-tailed unpaired *t* test (PR, sinus node recovery time, sinus cycle length and atrio-ventricular Wenck interval), and Mann-Whitney *U* test (PQ and AVERP intervals).

ECG Parameters	WT (*n* = 19)	nNOS-KO (*n* = 18)	P value
RR Interval (ms)	125 .5 ± 11.1	131.4 ± 18.9	0.22
PQ Interval (ms)	37.65 ± 6.6	38.34 ± 5.7	0.74
Sinus node recovery time	162.1 ± 23.4	164.6 ± 31.4	0.79
Sinus cycle length	134.2 ± 15.5	137.2 ± 22.9	0.64
Atrio-ventricular Wenck interval	77.87 ± 6.9	79.20 ± 7.3	0.61
Atrio-ventricular effective refractory period	59.38 ± 12.1	56 ± 7.9	0.37

Table S4. Clinical and demographic characteristics of patients in SR and with paroxysmal AF. ACEI, angiotensin-converting enzyme inhibitor; AF, atrial fibrillation; ARB, angiotensin II receptor blocker; AVR, aortic valve replacement; CABG, coronary artery bypass surgery; CCB, calcium channel blocker; COPD, chronic obstructive pulmonary disease; MI, myocardial infarction; MVR, mitral valve replacement; SR, sinus rhythm. The χ^2 test was use to compare gender, smoking status, and medical history between groups; the unpaired *t* test was used to compare age and the Fisher's exact test for surgical procedures. .

Groups of comparison	**SR**	**Paroxysmal AF**	***P* value**
Total number patients, *n*	(*n* = 8)	(*n* = 8)	
Age, years (mean ± SD)	64±11	64±9	0.15
Men, n %	7 (88)	5 (63)	0.66
Surgical procedure, %			
CABG±AVR/MVR	8 (100)	6 (75)	0.73
AVR/MVR	0 (0)	2 (25)	0.47
Maze procedure	0 (0)	1 (13)	1.00
Medical history, n %			
Smoker/ex-smoker	4 (50)	5 (63)	0.79
Hypertension	6 (75)	3 (38)	0.65
Diabetes mellitus	3 (38)	0 (0)	0.10
Heart Failure	0 (0)	1 (13)	0.33
Previous MI	3 (38)	1 (13)	0.37
COPD/asthma	3 (38)	0 (0)	0.23
Medications, %			
Anticoagulants	1 (13)	5 (63)	0.16
Antiplatelets	7 (88)	2 (25)	0.17
β-blockers	7 (88)	6 (75)	0.83
Statins	7 (88)	4 (50)	0.48
CCB	2 (25)	1 (13)	0.60
ACEIs and ARBs	5 (63)	3 (38)	0.56
Diuretics	2 (25)	1 (13)	0.60

Table S5. Clinical characteristics and demographics of patients in SR before and after surgery and of those who developed postoperative AF. ACEI, angiotensin-converting enzyme inhibitor; AF, atrial fibrillation; ARB, angiotensin II receptor blocker; AVR, aortic valve replacement; CABG, coronary artery bypass surgery; CCB, calcium channel blocker; COPD, chronic obstructive pulmonary disease; MI, myocardial infarction; MVR, mitral valve replacement; SR, sinus rhythm. The χ^2 test was use to compare gender, smoking status, and medical history between groups; the unpaired *t* test was used to compare age and the Fisher's exact test for surgical procedures.

Groups of comparison	**SR**	**Postoperative AF**	***P* value**
Total number patients, *n*	(*n* = 17)	(*n* = 18)	
Age, years (mean ± SD)	67±12	68±10	0.79
Men, n %	78	76	0.97
Surgical procedure, %			
CABG±AVR/MVR	72	76	1.00
AVR/MVR	28	24	1.00
Maze procedure	0	0	
Medical history, n %			
Smoker/ex-smoker	56	71	0.57
Hypertension	61	76	0.60
Diabetes mellitus	17	35	0.41
Heart Failure	11	35	0.23
Previous MI	39	18	0.23
COPD/asthma	11	12	1.00
Medications, %			
Anticoagulants	17	6	0.32
Antiplatelets	83	76	0.91
β-blockers	78	59	0.55
Statins	89	76	0.80
CCB	17	18	0.95
ACEIs and ARBs	61	76	0.60
Diuretics	56	71	0.57

Table S6. Predicted conserved (site 1) and poorly conserved (sites 2, 3, 4 and 5) miR-31 binding sites on the human *nNOS* 3'UTR. Seed region is shown in red.

Binding site	Conserved and poorly conserved sites	Predicted consequential pairing of target region of human *nNOS* 3'UTR (top) and miR-31-5p (bottom)	Seed match
Site 1	Position 9-15 of NOS1 3' UTR hsa-miR-31-5p	5' –NNNNNNNNCUGGACCCUCUUGCCC– 3' 3' –UCGAUACGGUCGUAGAACGGA– 5'	7mer-m8
Site 2	Position 254-260 of NOS1 3' UTR hsa-miR-31-5p	5' –UGUUCCCACUCCCUCUCUUGCCG– 3' 3' –UCGAUACGGUCGUAGAACGGA– 5'	7mer-m8
Site 3	Position 4371-4377 of NOS1 3' UTR hsa-miR-31-5p	5' –AAAUAAAAUAAAACAUCUUGCCC– 3' 3' –UCGAUACGGUCGUAGAACGGA– 5'	7mer-m8
Site 4	Position 4615-4621 of NOS1 3' UTR hsa-miR-31-5p	5' –UUGAAAGAGGUCAGGUCUUGCCC– 3' 3' –UCGAUACGGUCGUAGAACGGA– 5'	7mer-m8
Site 5	Position 4750-4757 of NOS1 3' UTR hsa-miR-31-5p	5' –AUGCAGCCUUUUCAUUCUUGCCA– 3' 3' –UCGAUACGGUCGUAGAACGGA– 5'	8mer

Table S7. Sequences of the miR-31-5p mimic, miR-31-5p hairpin inhibitor (α-miR-31), target site blockers (TSB) and negative controls with the binding sites for miR-31 on the human dystrophin (DYS) and nNOS (site 5) 3'UTR.

Name	Sequence (5' to 3')	miRBase accession number	Manufacturer (catalogue #)
miRIDIAN hsa-miR-31-5p mimic	AGGCAAGATGCTGGCATAGCT	MIMAT0000089	Dharmacon (C-300507)
miRIDIAN microRNA mimic negative control #1	TCACAACCTCCTAGAAAGAGTAGA	MIMAT0000039	Dharmacon (CN-001000)
miRIDIAN hsa-miR-31-5p hairpin inhibitor	TCCGTTCTACGACCGTATCGA		Dharmacon (C-300507)
miRIDIAN microRNA hairpin Inhibitor negative control #1	TCACAACCTCCTAGAAAGAGTAGA	MIMAT0000039	Dharmacon (IN-001005-01)
LNA_TSB_nNOS(site5)_ hsa-miR31-5p	TGGCAAGAATGAAAAGGC		Exiqon
Negative control for LNA_TSB_ nNOS(site5)_hsa-miR31-5p	TGACAGGAATGGAAAAGC		Exiqon
LNA_TSB_ dystrophin_hsa-miR31-5p	GGCAAGTTATTTAGCTAT		Exiqon
Negative control for TSB_ Dystrophin_ hsa-miR31-5p	TAACACGTCTATACGCCCA		Exiqon